Journal of Materials Chemistry B

Accepted Manuscript

ROYAL SOCIETY OF CHEMISTRY

www.rsc.org/materialsB

Table of Contents (TOC)

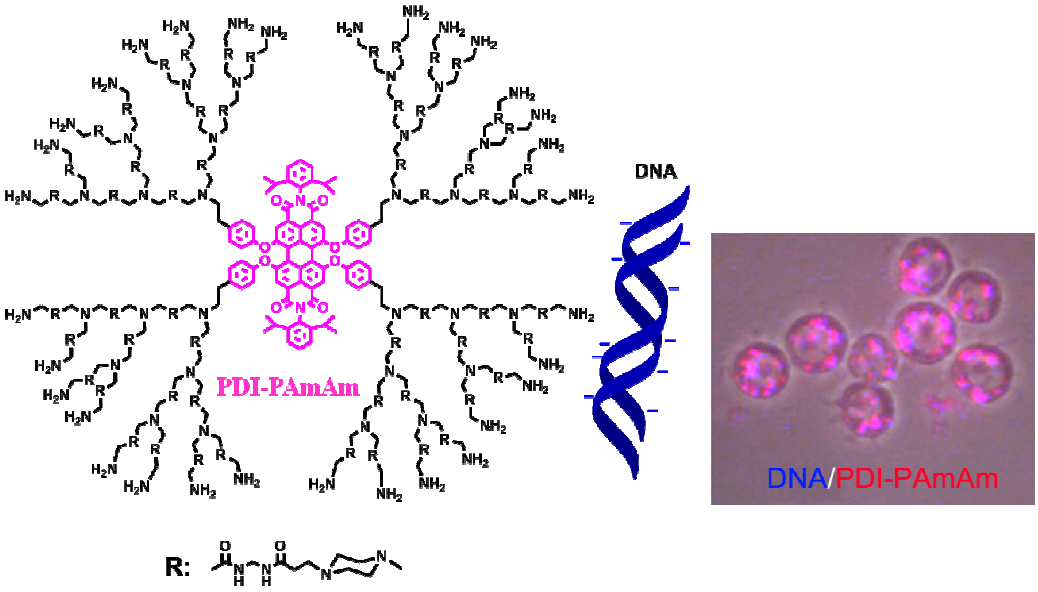

Journal of

Materials Chemistry B

RSCPublishing

ARTICLE

Highly water-soluble perylenediimide-cored poly(amido amine) vector for efficient gene transfection

Cite this: DOI: 10.1039/x0xx00000x

Received 00th January 2012,
Accepted 00th January 2012

DOI: 10.1039/x0xx00000x

www.rsc.org/

Zejun Xu,[a] Bicheng He,[b] Wei Wei,[b] Kelan Liu,[a] Meizhen Yin,*[a] Wantai Yang[a] and Jie Shen*[b]

Highly water-soluble perylenediimide-cored poly(amido amine) (PDI-PAmAm) with peripheral amine groups has been synthesized. The central PDI chromophore allows the optical monitoring of relevant cellular experiments by fluorescence microscopy. The PAmAm shell provides the steric bulk that notably suppresses the aggregation of the central PDI chromophore in aqueous solution. The peripheral amines provide water solubility and positive charges, and also serve as active sites for the further growth of PAmAm. PDI-PAmAm can be rapidly internalized into live cells with high efficacy of gene delivery and low cytotoxicity. Both *in vitro* and *in vivo* experiments demonstrate high gene transfection efficacy of PDI-PAmAm.

Introduction

Perylenediimides (PDIs) are an attractive class of fluorophores because of their exceptional chemical, thermal, and photochemical stability, and high fluorescence quantum yields in organic solvents.[1, 2] However, the poor solubility and very weak fluorescence of PDIs in an aqueous environment[3] have hindered their utilization in the biological and medicinal fields. Hydrophilic moieties have been incorporated in the bay region or at the imide positions to increase the water solubility of PDIs.[4-7] In general, the substituents in the bay regions of PDIs have the advantage of a significant red shift in the absorption maximum, and also with a larger Stokes shift. These shifts have attracted great interest as the interference from cell auto-fluorescence is minimized.[8-10] Another hydrophilic modification of PDIs is the attachment of water-soluble topological macromolecules (such as star polymers,[11-14] dendrimers,[15-19] or hyperbranched polymers[20]) to the PDI core. Compared with linear polymers, the branched polycations have a great number of functional groups, and exhibit low cytotoxicity and high transfection efficiency because of their globular structures.[19, 21, 22] The most reported PDI-cored dendrimers are neutral, water-soluble, and biocompatible in character.[15-18] PDI-cored cationic polyester dendrimers[19] have been reported by our group. The outer dendritic polyester units are not stable under basic condition; thus, the dendrimers have to be treated with diluted HCl to yield their ammonium salts.[19] The hydrophobic nature of outer polyesters leads to the relatively low water solubility of the previous PDI-cored dendrimers. Therefore, in this present work, highly water-soluble poly(amido amine) (PAmAm) dendritic units are incorporated into the bay regions of PDIs. Cationic PAmAm dendrimers exhibit good transfection efficiency and low cytotoxicity.[23] Additionally, the well-defined geometry of PAmAm dendrimer allows the ease of modification to increase their efficiency.[24, 25] The structure of PDI-cored poly(amido amine) (PDI-PAmAm) is given in **Scheme 1**. The water solubility and chemical stability of PDI-PAmAm are dramatically higher than those of the previous cationic polyester dendrimers[19] at all pH values. The central PDI chromophore allows the optical monitoring of relevant cellular experiments by fluorescence microscopy.[13, 19, 26] The PAmAm shell provides the steric bulk that notably suppresses the aggregation of the central PDI chromophore. The peripheral amines provide water solubility and positive charges, and also serve as active sites for the further growth of PAmAm. The optical properties of PDI-PAmAm in water were investigated. The cell-penetrating ability and the gene transfection efficacy of PDI-PAmAm were assayed both *in vitro* and *in vivo*.

Experimental section

Materials

Triethylamine (Et_3N, 99.5%), 2,6-diisopropylaniline (90+%), N-methyl-2-pyrrolidone (NMP, 99+%), 1-(2-aminoethyl) piperazine

(AEPZ, 98%), N,N'-methylene bisacrylamide (MBA, 99%) were purchased from Alfa Aesar and used without further purification. 1, 6, 7, 12-Tetrachloroperylene-3, 4, 9, 10-tetracar-boxylic acid dianhydride was obtained from Beijing Wenhaiyang Perylene Chemistry (Beijing, China). All other solvents and reagents were purchased from commercial suppliers and were used as received. S2 cells were propagated in Schneider Drosophila Medium supplemented with 10% FBS, 100 U/mL penicillin and 100 μg/mL streptomycin at 25 ^{o}C without CO_2.

Synthesis of compound 1

Compound **1** was synthesized according to the literature.[27] ^{1}H-NMR (400 MHz, CF_3COOD) δ 8.49 (s, 4H, *perylene*), 7.59 (d, *J* = 7.8 Hz, 2H, *Ph-H*), 7.46 (d, *J* = 7.9 Hz, 4H, *Ph-H*), 7.32 (d, *J* = 8.2 Hz, 8H, *Ph-H*), 7.19 (d, *J* = 8.3 Hz, 8H, *Ph-H*), 3.59 (s, 8H, CH_2), 3.18 (s, 8H, CH_2), 2.78-2.70 (m, 4H, *CH*), 1.21 (d, *J* = 6.4 Hz, 24H, CH_3 *isopropyl*). ^{13}C-NMR (151 MHz, CF_3COOD) δ 166.20, 156.75, 154.77, 145.53, 132.62, 131.81, 130.91, 130.28, 128.46, 124.87, 122.15, 121.42, 121.08, 120.76, 120.13, 42.01, 31.95, 29.08, 22.40.MS (MALDI-TOF, m/z) Calc. for $C_{80}H_{78}N_6O_8$: 1251.51, found: 1250.7.

Synthesis of PDI-PAmAm

PDI-PAmAm is synthesized via Michael addition copolymerization (Scheme 1 and S1).[28-30]

Synthesis of intermediate product 2

Compound **1** (200.0 mg, 0.16 mmol) and MBA (246.5 mg, 1.6 mmol) were added into a vial and dissolved in methanol/water mixture (6.0 mL, 8/2 v/v) at room temperature under an N_2 atmosphere. The reaction was carried out at 50 ^{o}C for 48 h. After cooling down to room temperature, the solution was washed with ether/hexane (4:1, v/v) (50 mL × 3). The residue was dried under vacuum to give a red solid intermediate product **2** in 95% yield. ^{1}H NMR (400 MHz, DMSO) δ 8.62 (d, *J* = 51.8 Hz, 16H, *NH*), 7.94 (s, 4H, *perylene*), 7.43 (s, 2H, *Ph-H*), 7.25 (d, *J* = 17.3 Hz, 12H, *Ph-H*), 6.98 (d, *J* = 11.8 Hz, 8H, *Ph-H*), 6.17 (d, *J* = 45.1 Hz, 16H, $\underline{CH_2}$=*CHCO*), 5.59 (s, 8H, CH_2=$\underline{CH}$*CO*), 4.45 (s, 16H, *NH*$\underline{CH_2}$*NH*), 3.38 (t, 16H, NCH_2), 2.70 (m, 20H, CH_2 *& CH*), 2.24 (t, 16H, CH_2), 1.01 (d, 24H, CH_3 *isopropyl*). ^{13}C NMR (151 MHz, DMSO) δ 171.89, 170.86, 164.87, 162.76, 155.69, 152.68, 145.44, 137.25, 137.08, 131.42, 130.44, 130.16, 129.30, 125.79,123.72, 122.41, 119.85, 119.58, 68.06, 57.76, 54.47, 49.19, 43.18, 39.52, 35.58, 33.02, 32.06, 28.31, 23.72. MS (MALDI-TOF, m/z) Calc. for $C_{136}H_{158}N_{22}O_{24}$: 2484.84, found: 2485.47($M+H^+$), 2507.74 ($M+Na^+$).

Synthesis of intermediate product 3

Then, the intermediate product **2** (248.5 mg, 0.1 mmol) and AEPZ (129.0 mg, 1.0 mmol) were dissolved in methanol/water mixture (6.0 mL, 8/2 v/v). The solution was stirred at room temperature under N_2 atmosphere for 5 h, and then stirred at 50 ^{o}C for 56 h. After cooling down to room temperature, the solution was washed with ether/hexane (6:1, v/v) (50 mL × 3). The residue was dried under vacuum to give a red solid intermediate product **3** in 88% yield. ^{1}H NMR (600 MHz, DMSO) δ 8.53 (d, *J* = 32.0 Hz, 16H, *NH*), 7.95 (s, 4H, *perylene*), 7.40 (s, 2H, *Ph-H*), 7.26 (d, *J* = 38.3 Hz, 12H, *Ph-H*), 6.94 (d, *J* = 28.6 Hz, 8H, *Ph-H*), 4.34 (s, 16H, *NH*$\underline{CH_2}$*NH*), 3.39 (t, 32H, NCH_2), 2.69-2.21 (m, 152H, CH_2 *& CH*), 1.01 (d, 24H, CH_3 *isopropyl*). ^{13}C NMR (101 MHz, DMSO) δ 171.80, 170.62, 165.93, 162.87, 155.62, 152.65, 145.52, 137.24, 137.06, 130.45, 130.23, 129.18, 123.71, 122.36, 119.89, 119.50, 68.04, 64.83, 60.62, 57.75, 54.65, 53.76, 52.80, 52.44, 49.20, 45.48, 43.05, 35.56, 33.01, 32.77, 32.04, 28.29, 23.71. MS (MALDI-TOF, m/z) Calc. for $C_{184}H_{278}N_{46}O_{24}$: 3518.47, found: 3519.15($M+H^+$), 3390.41 (M-AEPZ), 3258.12 (M-2AEPZ).

Synthesis of intermediate product 3b

Compound **3** (281.4 mg, 0.08 mmol) and MBA (295.6 mg, 1.92 mmol) were added into a vial and dissolved in methanol/water mixture (6.0 mL, 8/2 v/v) at room temperature under an N_2 atmosphere. The reaction was carried out at 50 ^{o}C for 60 h. After cooling down to room temperature, the solution was washed with ether/hexane (4:1, v/v) (60 mL × 3). The residue was dried under vacuum to give a red solid intermediate product **3b**. ^{1}H NMR (400 MHz, MeOD) δ 8.13 (s, 4H, *perylene*), 7.47 (s, 2H, *Ph-H*), 7.22 (m, 12H, *Ph-H*), 7.03 (s, 8H, *Ph-H*), 6.27 (d, *J* = 5.7 Hz, 32H, $\underline{CH_2}$=*CHCO*), 5.71 (d, *J* = 6.0 Hz, 16H, CH_2=$\underline{CH}$*CO*), 4.63 (m, 48H, *NH*$\underline{CH_2}$*NH*), 3.34 (m, 64H, NCH_2), 2.75-2.40 (m, 216H, CH_2 *& CH*), 1.10 (d, 24H, CH_3 *isopropyl*). ^{13}C NMR (151 MHz, MeOD) δ 175.27, 174.19, 168.21, 164.87, 154.75, 152.85,147.16, 139.15, 138.60, 131.83, 131.63, 130.60, 129.54, 127.61, 126.11, 125.05, 123.78, 121.81, 121.46, 120.45, 69.47, 67.01, 58.94, 54.22, 51.03, 45.20, 37.27, 35.37, 34.45, 30.90, 24.37, 21.33. MS (MALDI-TOF, m/z) Calc. for $C_{296}H_{438}N_{78}O_{56}$: 5985.13, found: 5870.21 (M-MBA+K^+), 5853.95 (M-MBA+Na^+), 5715.26 (M-2MBA+K^+), 5700.07 (M-2MBA+Na^+).

Synthesis of intermediate product 4

Intermediate product **4** was synthesized by using compound **3b** and AEPZ (309.6 mg, 2.4 mmol) according to the same procedure as the previous synthesis of compound **3**. Compound **4** was received as a red solid. ^{1}H NMR (400 MHz, MeOD) δ 8.15 (s, 4H, *perylene*), 7.45 (s, 2H, *Ph-H*), 7.38-7.16 (m, 12H, *Ph-H*), 7.03 (s, 8H, *Ph-H*), 4.56 (s, 48H, *NH*$\underline{CH_2}$*NH*), 3.33 (t, 96H, NCH_2), 2.72-2.37 (m, 408H, CH_2 *& CH*), 1.13 (d, 24H, CH_3 *isopropyl*). ^{13}C NMR (151 MHz, MeOD) δ 175.24, 174.75, 174.15, 164.90, 157.69, 154.75, 147.15, 138.63, 134.45, 131.62, 131.45, 130.64, 125.05, 123.80, 121.45, 121.22, 120.02, 69.48, 58.95, 54.94, 53.83, 53.63, 50.75, 46.20, 45.09, 38.13, 37.27, 35.75, 34.44, 33.74, 30.32, 24.39. MS (MALDI-TOF, m/z) Calc. for $C_{392}H_{678}N_{126}O_{56}$: 8052.39, found: 7523.39.15 (M-2(MBA+AEPZ)+K^+), 7261.52 (M-3(MBA+AEPZ)+Na^++K^+).

Synthesis of intermediate product 4b

Compound **4b** was synthesized by using intermediate product **4** (483.1 mg, 0.06 mmol) and MBA (369.6 mg, 2.4 mmol) according to the same procedure as the previous synthesis of compound **2.** Compound **4b** was received as a red solid. ^{1}H NMR (400 MHz, MeOD) δ 8.13 (s, 4H, *perylene*), 7.47 (s, 2H, *Ph-H*), 7.22 (s, 12H, *Ph-H*), 7.03 (s, 8H, *Ph-H*), 6.27 (d, *J* = 5.8 Hz, 64H, $\underline{CH_2}$=*CHCO*), 5.71 (d, *J* = 5.7 Hz, 32H, CH_2=$\underline{CH}$*CO*), 4.67 (m, 112H, *NH*$\underline{CH_2}$*NH*), 3.34 (m, 162H, NCH_2), 2.77-2.39 (m, 476H, CH_2 *& CH*), 1.14 (d, 24H, CH_3 *isopropyl*). ^{13}C NMR (151 MHz, MeOD) δ175.29, 174.99,

174.21, 168.23, 164.96, 154.79, 147.17, 138.63, 134.43, 131.82, 131.63, 130.65, 127.74, 125.06, 123.77, 121.87, 121.46, 120.39, 69.48, 58.92, 56.89, 54.80, 54.09, 53.15, 51.08, 45.19, 37.27, 34.36, 33.73, 33.62, 30.31, 24.38. GPC: Mw, 7.1×10^3 Da; PD, 1.01.

Synthesis of final product PDI-PAmAm

PDI-PAmAm was synthesized by using compound **4b** and AEPZ (495.4 mg, 3.84 mmol) according to the same procedure as the previous synthesis of compound **3.** PDI-PAmAm was received as a red solid in 90% yield. The chemical structure of PDI-PAmAm was characterized by ^{1}H NMR and ^{13}C NMR using a Bruker spectrometer. ^{1}H NMR (400 MHz, D_2O) δ 8.48 (s, 4H, *perylene*), 7.98 (s, 2H, *Ph-H*), 7.73 (s, 12H, *Ph-H*), 7.66 (d, 8H, *Ph-H*), 4.54 (s, 112H, *NHCH$_2$NH*), 3.34 (m, 224H, *NCH$_2$*), 2.84-2.46 (m, 900H, *CH$_2$ & CH*), 1.16 (d, 24H, *CH$_3$ isopropyl*). ^{13}C NMR (101 MHz, DMSO) δ 171.87, 171.56, 170.53, 162.69 , 155.42, 152.84, 145.58, 137.14, 132.58, 130.63, 130.40, 130.26, 123.54, 122.07, 119.71, 118.55, 67.93, 57.46, 54.52, 52.63, 52.44, 52.33, 49.74, 48.91, 45.23, 43.14, 37.04, 35.88, 33.00, 32.77, 32.02, 28.59, 23.86. GPC: Mw, 1.0×10^4 Da; PD, 1.04.

Characterization

Nuclear magnetic resonance (NMR) spectra were recorded on Bruker 400 (400 MHz ^{1}H; 100 MHz ^{13}C) or Bruker 600 (600 MHz ^{1}H; 150 MHz ^{13}C) spectrometer using D_2O, MeOD, DMSO and CF_3COOD as solvent at room temperature. Chemical shifts were reported downfield from 0.00 ppm using TMS as internal reference. Matrix-assisted laser-desorption ionization time-of-flight mass spectrometry (MALDI-TOF MS) were determined on Bruker Daltonics Inc. BIFLEX III MALDI-TOF mass spectrometer. Number-average (Mn) and weight-average (Mw) molecular weights and polydispersity index (Mw/Mn, PD) of **4b** and PDI-PAmAm were determined by gel penetration chromatograph (GPC) (Agilent 2600 Series) with dimethyl formamide (DMF) as the mobile phase. The column model was PLgel 5 μm 10^3Å, the flow rate of mobile phase was set to be 1 mL/min, and the temperature of both column and detector was 25 °C. The standard curve was determined using a series of narrow distribution polystyrene standard samples. The UV-Vis absorption spectra were recorded on a spectrophotometer (Cintra 20, GBC, and Australia). The corrected fluorescence spectroscopic studies were performed on a fluorescence spectrophotometer (Horiba Jobin Yvon FluoroMax-4 NIR, NJ, USA) at room temperature (25 ^{o}C). Fluorescence quantum yields ($Ø_f$) were measured at room temperature by using cresyl violet in methanol as reference.[5]

Characterization of PDI-PAmAm/DNA complexes

The purity and concentration of the purified DNA were determined by absorption at 260 and 280 nm and by agarose gel electrophoresis. N/P ratios are expressed as molar ratios of nitrogen (N) in PDI-PAmAm to phosphate (P) in DNA. The average mass weight of 325 per phosphate group of DNA was assumed. All PDI-PAmAm/DNA complexes were formed by mixing equal volumes of PDI-PAmAm and DNA solutions to achieve the desired N: P ratio. Each mixture was vortexed and incubated for 30 min at room temperature. PDI-PAmAm was examined for its ability to bind DNA through agarose gel electrophoresis using the similar procedures to those described earlier.[14] The particle sizes and zeta potentials of PDI-PAmAm/DNA complexes were measured in triplicate using a Zetasizer Nano ZS (Malvern Instruments, Southborough, MA).

Cytotoxicity Assay

Cell viability was monitored using Tali™ viability kit-Dead Cell Green (Invitrogen, Catalog A10787). The measurement was performed according to the manufacture's instruction. PEI, PDI-PAmAm and PDI-PAmAm/DNA complexes were separately added into culture medium to treat cells for 48 h. Then fresh cell medium containing Dead Cell Green (1:100 dilution) was used for additional 0.5 h incubation.

Cellular Uptake

Cellular uptake experiment was performed in 35 mm × 35 mm cell culture dish, 2.5×10^5 cells per well. After 6 h of cell seeding, the PDI-PAmAm was added into the cell culture dish. Cellular uptake was imaged under a fluorescent microscope. The fluorescence intensity of internalized PDI-PAmAm was calculated by Image-J Program.

DNA delivery

DNA fragment (20 bp, 100 μM) was labelled with 30 μM CXR Reference Dye (Promega, Catalog C5411) that could bind with DNA at a final concentration of 0.3-0.5 μM. DNA and PDI-PAmAm at different N/P ratios of 2:1, 4:1, and 8:1 were pre-incubated in culture medium at room temperature. Then the complex was added into culture medium to treat cells. After an incubation of 24 h, 36 h, and 48 h, the fluorescence image of PDI-PAmAm and DNA was obtained by fluorescent microscopy. PEI/DNA complexes were used as a control.

Gene transfection assay

Gene transfection assays were performed using plasmid pAc-GFP (323 ng/μL) as the reporter gene in S2 cell line. In brief, the cells were seeded in plates at a density of 2.5×10^5 cells in 1000 μL of fresh normal medium (supplemented with 10% FBS) per well in 35 mm × 35 mm cell culture dish and incubated for 5 h. We prepared the PDI-PAmAm/pDNA complexes at N/P ratio of 20 by adding the PDI-PAmAm to the DNA solutions, followed by incubation for 15 min at room temperature. At the time of transfection, the medium was replaced with serum-free medium. The PDI-PAmAm/pDNA complexes were added to the medium and incubated with the cells for 6 h under the standard incubation conditions. Then, the medium was replaced with 1500 μL of the fresh normal medium (supplemented with 10% FBS). The cells were further incubated for an additional 54 h under the same conditions, giving rise to a total transfection time of 60 h. Then GFP expression was detected using fluorescent microscopy. PEI/pDNA complexes at the N/P ratio of 20 were used as a control.

Insects raising

Drosophila larvae were fed with an artificial diet containing the gene carrier PDI-PAmAm from first to third instar, and then the guts of the third instar larvae were dissected and observed under a fluorescence microscope. Immediately after hatching from eggs,

Black cutworm larvae were picked out and individually fed with an artificial diet mixed with dsRNA alone or complex of dsRNA/PDI-PAmAm. The larval development status was imaged for analysis.

Gene carrier-delivered RNAi in insect

dsRNA targeting a key developmental gene *decapentaplegic* (*dpp*) were synthesized using T7 RiboMAX expression RNAi system (Promega). 12 μg of dsRNA were mixed with 12 μg of the gene carrier PDI-PAmAm, and then the complex was mixed with fresh artificial diet. The newly-hatched larvae were individually fed with this diet. The larvae fed with dsRNA alone were used as control experiment. After 4 days, dsRNA-contained food was replaced with fresh normal food. Then photos were taken for comparison.

The sequence of synthesized dpp-dsRNA is as following:
CAGAACATAATCATGGACTATTAGTGCGTGTGTTAGAAGA
GGGTGAGCAAAATATAGACGCTAAACAACCACATGTGAG
AGTGCGGAGACGTGCCGAGGAGGAGGAGGCCGAGTGGAG
CACGCGGCAACCTCTGCTGCTGCTGTACACGGAGGACGCG
CGCGCGCGCGCCGCTCGGGAGAGCGGAGAGACGCGGCTG
GTTCGCAACAAGCGCGCGACGCAGCGGCGTGGTCATCGAG
CACATCACCGCCGCAAGGAGGCGCGCGAGATCTGCCAGC
GACGTCCGCTCTACGTGGACTTCGCGGAGGTGGGCTGGAG
CGATTGGATCGTGGCGCCGCACGGCTACGAGGCGTACTAC
TGCCAGGGCGACTGCCCGTTCCCGCTGGCCGACCACCTCA
ACGGCACGAACCACGCGATCGTGCAGACTCTCGTGAACTC
AGTGAACCCGGCCGCAGTGCCGAAAGCGTGCTGTGTACCG
ACACAGCTCTCCTCTATTTCCAT

Results and discussion

Synthesis

The detailed synthesis procedures and material characterizations can be found in experimental section and the Electronic Supplementary Information (**ESI**†). Amine-functionalized PDI (**1**, Scheme 1) was prepared according to the literature.[27] The four primary amines in dye **1** reacted with one acrylamide group in excess N,N'-methylene bisacrylamide (**1**:MBA=1:10) via a Michael addition reaction to form vinyl-functionalized intermediate product **2**[28-30] to ensure the completion of the reaction, as monitored by MALDI-TOF MS spectrometry and ^{1}H NMR spectra (Fig. S7 and S8, **ESI**†). Repeated washing with ether/hexane (4:1, v/v) yielded pure **2**. The acrylamides at the periphery of **2** selectively reacted with the secondary amine group in excess 1-(2-aminoethyl) piperazine (AEPZ) (**2**: AEPZ=1:10) by a Michael addition resulting in **3**.[29] The characteristic peaks of the methylene group (CH_2=) at 5.59, 6.11, and 6.23 ppm disappear completely (Fig. 1), indicating the completion of the Michael addition of acrylamides in compound **2**. Repeated washing with ether/hexane (6:1, v/v) to remove the unreacted AEPZ. Similarly, alternately adding MBA and APEZ into the reaction system produced amine-functionalized intermediate product **4** and desired product PDI-PAmAm. PDI-PAmAm contains dendritic polyamide units and shows high water solubility (> 20 mg/mL), chemical stability without treatment with HCl. The fluorescence intensity of PDI-PAmAm in aqueous solution remained nearly unchanged after 24 h exposure under natural light (Fig. S1, **ESI**†), suggesting its good photostability. The high water solubility and photostability are essential properties for biological applications.

Optical properties of PDI-PAmAm

The aggregation behavior of PDI-PAmAm in aqueous solution was studied by the concentration-dependent UV-Vis absorption spectroscopy (Fig. 2(A)). The absorption bands of PDI-PAmAm show the characteristic π-π* transitions at 455, 554 and 596 nm, consistent with those of the bay-modified PDIs.[4, 17] The absorption spectra of aqueous solutions of PDI-PAmAm in the concentration range 0.2 μM to 2.0 μM exhibit the same absorption peak as the PDI chromophore core. A linear concentration-dependent absorbance is observed over the whole concentration range studied (Fig. 2(A), inset), implying that PDI-PAmAm exists in a typically monomeric form in the concentration range studied. The concentration-dependent fluorescence behaviour of PDI-PAmAm in water at the excitation wavelength 554 nm was also investigated (Fig. 2(B)). PDI-PAmAm retains the characteristic emission properties of bay-region substituted PDIs and exhibits an emission peak at 631 nm. Even when the concentration of PDI-PAmAm in water is as high as 2.0 μM, the maximum emission peak is almost unshifted and no new emission peaks are observed, indicating that the aggregation of the central PDI in aqueous solution was inhibited by PAmAm. The fluorescence quantum yield ($Ø_f$) of aqueous PDI-PAmAm was 0.18, obtained by using Cresyl Violet with a $Ø_f$ of 0.54 in methanol as a reference chromophore.[5] The above results indicate that PAmAm shell encapsulates the PDI chromophore and clearly improves the water solubility of PDI by suppressing aggregation in water. These characterizations make PDI-PAmAm as a useful candidate in bioapplications such as cell uptake and gene transfection.

PDI-PAmAm/DNA complexes

For cellular transfection, PDI-PAmAm and DNA have to form a stable complex in solution. Gel retardation test at various N/P ratios of PDI-PAmAm/DNA complexes was performed to determine whether the complexes are stable. As shown in Fig.3, PDI-PAmAm can prevent DNA band from moving in the gel at an N/P ratio of above 1. PDI-PAmAm can efficiently compact DNA into small nanoparticles, as shown in Table S1 (**ESI**†). In general, the hydrodynamic size of the complex decreases with increasing N/P ratio. And PDI-PAmAm can condense DNA into nanoparticles of various diameters in the range 100 - 200 nm at an N/P ratio of above 2. Zeta potential is an indicator of surface charges on the polymer/DNA nanoparticles. A positively charged surface allows electrostatic interaction with anionic cell surfaces and facilitates cellular uptake. The zeta-potential of PDI-PAmAm before and after it form a complex with DNA at various N/P ratios are presented in Table S2 (**ESI**†). The zeta potentials of PDI-PAmAm/DNA complex

increased with the increase of N/P ratios, indicating the efficient binding of PDI-PAmAm and DNA.

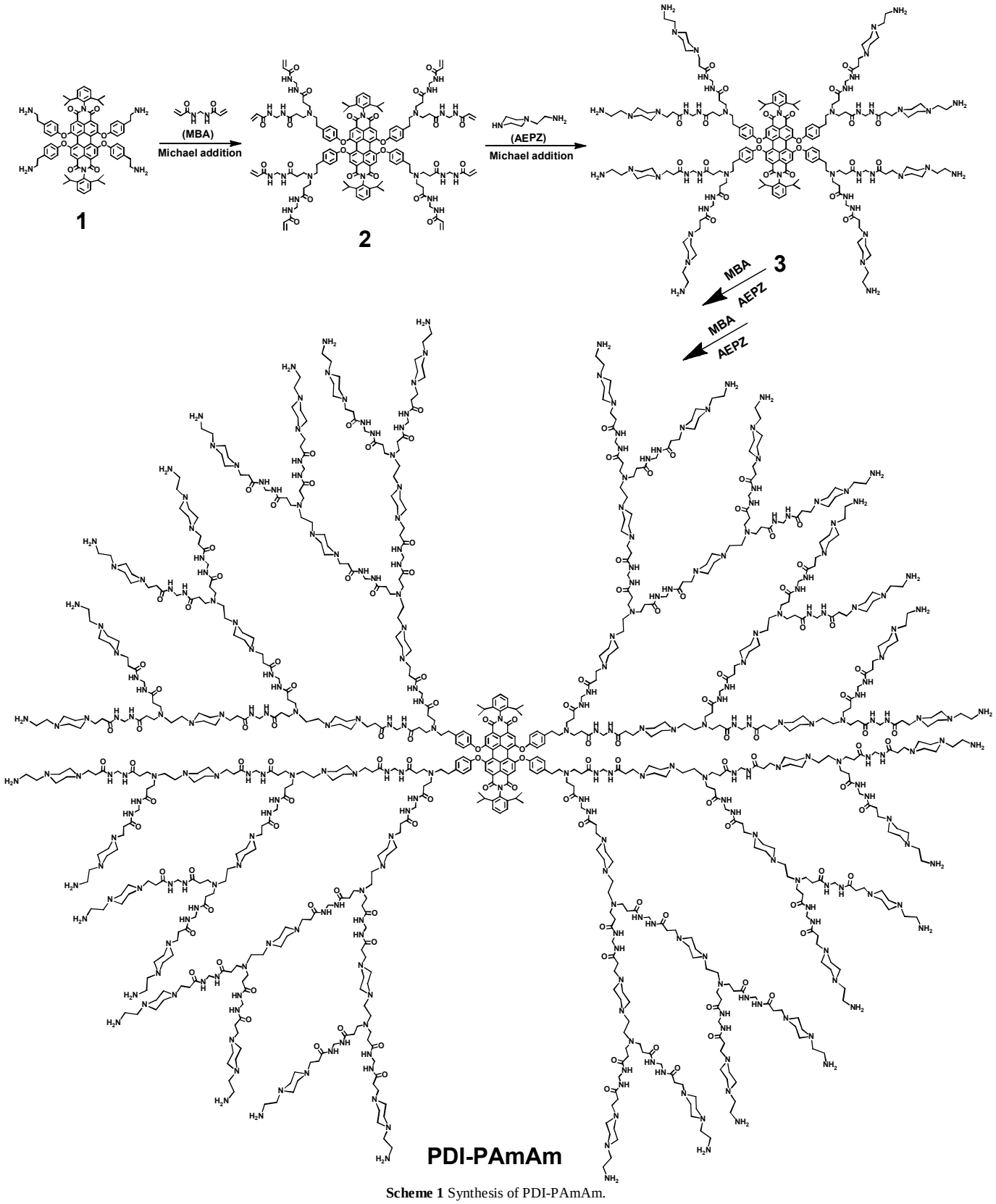

Scheme 1 Synthesis of PDI-PAmAm.

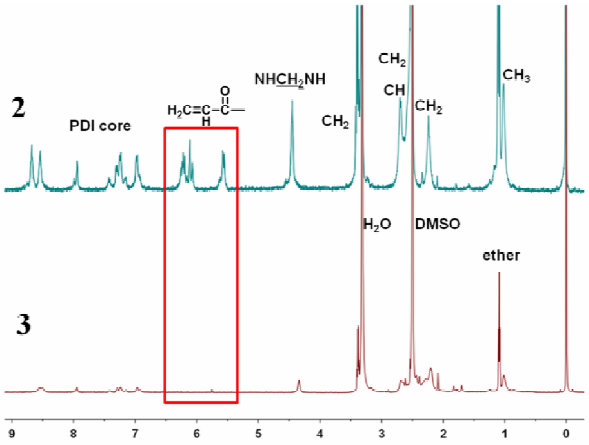

Fig. 1 ^{1}H NMR spectra of the intermediate product **2** and **3** in DMSO (Note: the characteristic peaks of methylene group (CH_2=) at 5.59, 6.11 and 6.23 ppm disappeared completely, indicating the completion of the Michael addition of acrylamides in **2**).

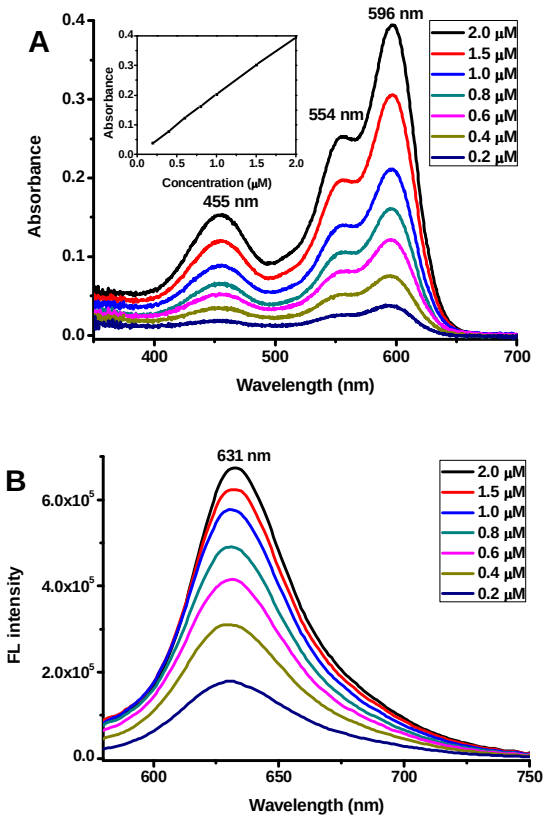

Fig. 2 Concentration-dependent (A) absorbance and (B) fluorescence (FL) spectra of PDI-PAmAm in water (concentration: 0.2 μM to 2.0 μM, λ_{ex} = 554 nm). Inset: dependence of absorbance intensity (at λ_{max} of 596 nm) on concentration.

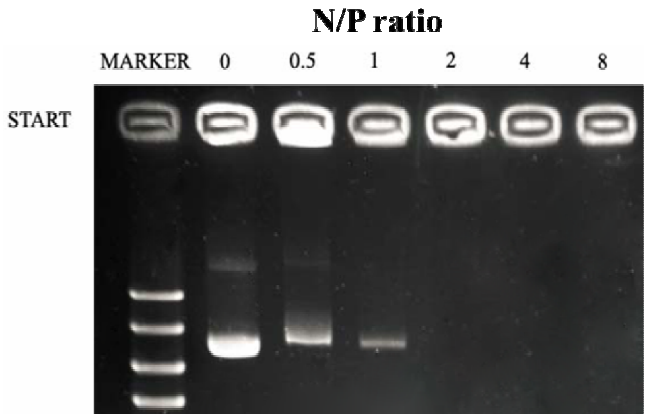

Fig. 3 Agarose gel electrophoresis of PDI-PAmAm/DNA complexes at various N/P ratios.

Cytotoxicities of PDI-PAmAm and PDI-PAmAm/DNA complexes

It is very important to evaluate the potential toxicity of polymeric materials for biomedical applications. Here, the *in vitro* cytotoxicity of PEI, PDI-PAmAm and PDI-PAmAm/DNA complexes were assessed by Tali™ viabilty assay[13, 19] using *Drosophila* S2 cells. As shown in Fig.4, the cell viabilities of PDI-PAmAm are higher than 92% at all the concentrations studied. This cell viability of PDI-PAmAm is comparable with the value of previous reported cationic dendrimers[19] and is better than that of previous reported fluorescent nanoparticle,[13] indicating that the PDI-PAmAm solutions at these concentrations have low toxicity. The cell viabilities of PDI-PAmAm/DNA complexes are still high (>91%) as shown in Fig. 4. Both pure PDI-PAmAm and PDI-PAmAm/DNA complexes exhibit much lower toxicity than the commercial gene carrier PEI (1μM) does (Fig. 4). The cell viability of PEI is consistent with the results reported in the literature.[21]

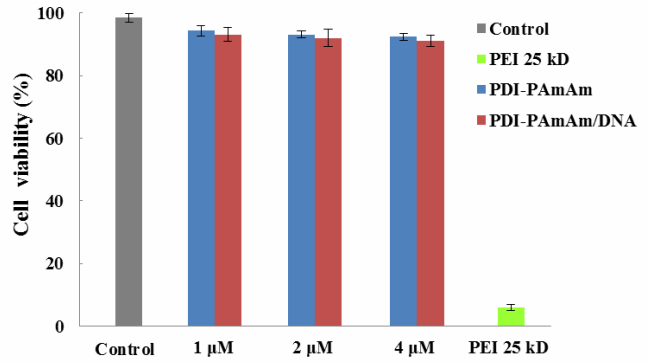

Fig. 4 Cell viability assays.

Gene transfection

To investigate the ability of PDI-PAmAm to enter into live cells, *Drosophila* S2 cells were incubated with PDI-PAmAm. Because of the central PDI chromophore, the distributions of PDI-PAmAm in live cells can be traced by fluorescence microscopy. The detectable fluorescent signal depends on PDI-

PAmAm concentration. As shown in Fig. 5(C), PDI-PAmAm can be detected inside the cells after an incubation of approximately 1 h at a concentration of 2 μM, demonstrating the efficient and rapid internalization of PDI-PAmAm. While previous reported cationic polyester dendrimers[19] required higher concentration to be detected inside live cells (Fig. 5(C)). Therefore, the outer PAmAm shell structure contributes to the enhanced cellular internalization of PDI-PAmAm.

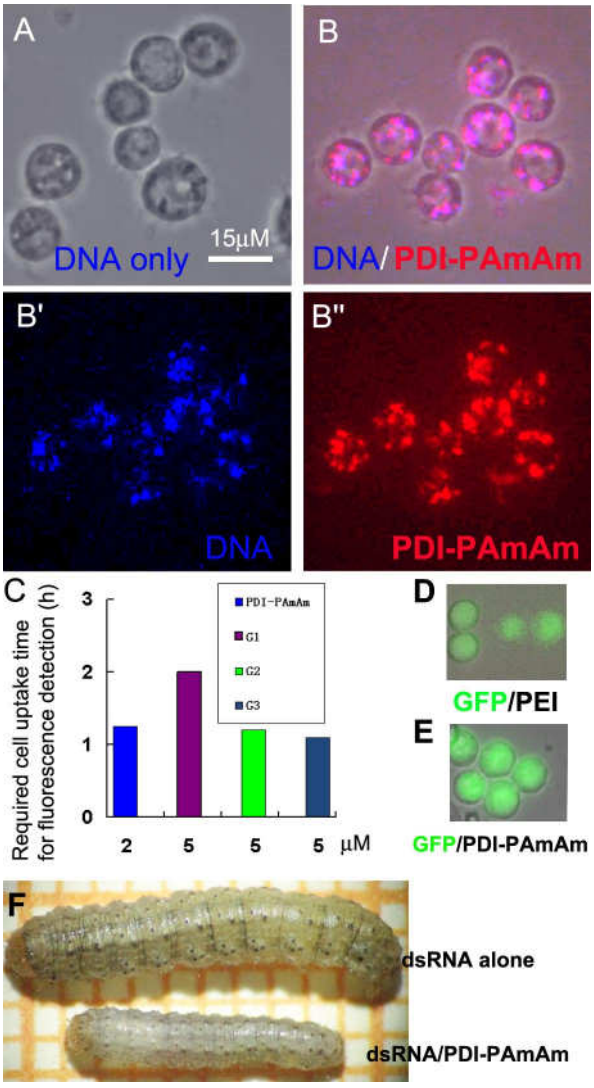

Fig. 5 Gene transfection assays of PDI-PAmAm. (A) Control experiment. DNA alone cannot enter into live cells. (B) Fluorescence images of PDI-PAmAm/DNA complex internalized into live cells (2 μM PDI-PAmAm, 100 μM DNA, N/P = 8:1). Separated channels are shown in (B') (red, PDI-PAmAm) and (B'') (blue, DNA). DNA was fluorescently labelled by CXR Reference Dye (blue). (C) Required incubation time (h) of PDI-PAmAm and previous reported Gs for fluorescence detection. (D) Relatively weak GFP expression of PEI delivered GFP plasmid in cells. (E) Much stronger GFP expression of PDI-PAmAm delivered GFP plasmid in cells. (F) After oral feeding with artificial diet containing PDI-PAmAm-delivered dsRNA targeting a key developmental gene *decapentaplegic*, larvae show apparent growth defects compared with the control.

The above results of cell uptake demonstrate that PDI-PAmAm can be rapidly internalized into live cells within a short incubation time. The positive charges in PDI-PAmAm can interact with negatively charged macromolecules such as DNA through electrostatic forces.[31-33] In order to assess whether PDI-PAmAm can act as a carrier for delivering DNA into cells, live S2 cells were incubated with a buffer containing PDI-PAmAm/DNA complexes at N/P ratios of 2:1, 4:1, and 8:1. In the control experiment, DNA alone cannot enter into live cells (Fig. 5(A)). The gene delivery efficacies of PDI-PAmAm/DNA complexes were visualized by fluorescent tracing of their cellular distribution of PDI-PAmAm and of DNA labelled by CXR Reference Dye (CRD). After 36 h incubation, both PDI-PAmAm and DNA are enriched in live cells, suggesting effective delivery by PDI-PAmAm (Fig. 5(B), (B') and (B'')). The gene delivery rate and efficacy of PDI-PAmAm are confirmed by the quantified fluorescence intensity of the CRD-labelled DNA inside the cells (Fig. S2 and S3, **ESI**†). The gene delivery efficacy of PDI-PAmAm is better than that of the previous reported fluorescent nanoparticle (FNP)[13] and cationic dendrimers[19] (Fig. S3(B)). The remarkable fluorescence intensity of CRD-labelled DNA at lower N/P ratios suggests the high gene delivery efficacy of PDI-PAmAm. While the commercial DNA carrier PEI requires high N/P ratios for gene delivery.[21] Under the same conditions, PDI-PAmAm delivering DNA into live cells is much faster than the commercial one (Fig. S4, **ESI**†).

To examine the efficacy of PDI-PAmAm for gene transfection *in vitro*, a GFP plasmid was chosen for further *in vitro* test. As shown in Fig. 5(D) and Fig. S5 (**ESI**†), the weak green fluorescence is observed in the cells in a control experiment of PEI-delivered GFP expression. As expected, strong green fluorescence is observed in the cells in the case of PDI-PAmAm-delivered GFP expression (Fig. 5(E) and Fig. S5(**ESI**†)). This suggests that PDI-PAmAm is an efficient gene carrier for *in vitro* applications.

To investigate the gene deliver efficacy of PDI-PAmAm under *in vivo* conditions, we firstly test whether PDI-PAmAm is able to enter into gut tissue of *Drosophila* larvae. First instar larvae were fed with fresh artificial diet containing PDI-PAmAm. After 3 days feeding, the larvae were dissected to obtain guts for fluorescence observation. As shown in Fig. S6 (A), the red fluorescent spots were observed in the gut cells, indicating that PDI-PAmAm passed through the peritrophic membrane and entered into the gut cells. All tested larvae survived to adult hood which demonstrates the safety of PDI-PAmAm-contained diet. Then we test whether PDI-PAmAm/dsRNA complex is able to enter into gut tissue. GFP-dsRNA fragment was synthesized with T7 RiboMAX expression RNAi system, and was labelled with a blue-fluorescence CRD. The dissected larval guts were incubated with PDI-PAmAm/dsRNA (at the N/P ratio of 2:1) complexes. The delivery of dsRNA by PDI-PAmAm was observed by the fluorescence distributions of PDI-PAmAm and the CRD labelled dsRNA in gut tissues (Fig. S6(B-B'')). For *in vivo* applications to interfere gene expression, dsRNA fragments

were synthesized for specific targeting a key developmental gene *decapentaplegic* (*dpp*)[34] of an insect pest, Black cutworm. After oral feeding with artificial diet containing PDI-PAmAm/dsRNA (at the N/P ratio of 2:1) complexes, the tested larvae showed apparent growth defects compared with the control of dsRNA alone (Fig. 5(F)) and the negative control of complexing GFP-dsRNA. After 4 days' treatment, the growth inhibition was quantified by measuring the larval body length. Compared with the larvae fed with dsRNA alone, the body length of PDI-PAmAm/dsRNA fed larvae reduced 35%, indicating an apparent growth defect induced by the complexes. These results demonstrate that PDI-PAmAm fulfils the requirements of gene carrier for both *in vitro* and *in vivo* applications.

Conclusions

In conclusion, the synthesis and optical properties of a novel water-soluble PDI-PAmAm are reported. The aggregation of the encapsulated PDI chromophore was noticeably suppressed by outer PAmAm shells, thus leading to the enhancement of optical performance of PDI in water. Strong red fluorescence, good water solubility, and high photostability were the prime attractions for bio-applications. PDI-PAmAm can be rapidly internalized into live cells, with high efficacy of gene delivery and low cytotoxicity. PDI-PAmAm shows great performance of gene transfection and gene interference in both *in vitro* and *in vivo* experiments.

Acknowledgements

This work was financially supported by the 973 Program (2013CB127603), the National Science Foundation of China (21174012, 51103008, 51221002, 31372255), Special Fund for Agro-scientific Research in the Public Interest (201003025), the New Century Excellent Talents Award Program from Ministry of Education (NCET-10-0215) and the Doctoral Program of Higher Education Research Fund (20120010110008).

Notes and references

[a] State Key Laboratory of Chemical Resource Engineering, Key Laboratory of Carbon Fiber and Functional Polymers, Beijing University of Chemical Technology, Ministry of Education, 100029 Beijing, China, Email: yinmz@mail.buct.edu.cn.

[b] Department of Entomology, China Agricultural University, 100193 Beijing, China, Email: shenjie@cau.edu.cn

† Electronic Supplementary Information (ESI) available: See DOI: 10.1039/b000000x/

1 M. D. Yilmaz, O. A. Bozdemir and E. U. Akkaya, *Org. Lett.*, 2006, **8**, 2871.

2 T. Weil, T. Vosch, J. Hofkens, K. Peneva and K. Müllen, *Angew. Chem. Int. Ed.*, 2010, **49**, 9068.

3 H. Langhals, W. Jona, F. Einsiedl and S. Wohnlich, *Adv. Mater.*, 1998, **10**, 1022.

4 J. Qu, C. Kohl, M. Pottek and K. Müllen, *Angew. Chem. Int. Ed.*, 2004, **43**, 1528.

5 C. Kohl, T. Weil, J. Qu and K. Müllen, *Chem. -Eur. J.*, 2004, **10**, 5297.

6 C. Backes, C. D. Schmidt, F. Hauke, C. Böttcher and A. Hirsch, *J. Am. Chem. Soc.*, 2009, **131**, 2172.

7 S. Rehm, V. Stepanenko, X. Zhang, T. H. Rehm and F. Würthner, *Chem. -Eur. J.*, 2010, **16**, 3372.

8 S. Demmig and H. Langhals, *Chem. Ber.*, 1988, **121**, 225.

9 H. Kobayashi, M. Ogawa, R. Alford, P. L. Choyke and Y. Urano, *Chem. Rev.*, 2009, **110**, 2620.

10 S. K. Yang and S. C. Zimmerman, *Adv. Funct. Mater.*, 2012, **22**, 3023.

11 M. Yin, J. Shen, G. O. Pflugfelder and K. Müllen, *J. Am. Chem. Soc.*, 2008, **130**, 7806.

12 M. Yin, J. Shen, R. Gropeanu, G. O. Pflugfelder, T. Weil and K. Müllen, *Small*, 2008, **4**, 894.

13 B. He, Y. Chu, M. Yin, K. Müllen, C. An and J. Shen, *Adv. Mater.*, 2013, **25**, 4580.

14 M. Yin, C. Feng, J. Shen, Y. Yu, Z. Xu, W. Yang, W. Knoll and K. Müllen, *small*, 2011, **7**, 1629.

15 T. Heek, C. Fasting, C. Rest, X. Zhang, F. Würthner and R. Haag, *Chem. Commun.*, 2010, **46**, 1884.

16 T. Heek, F. Würthner and R. Haag, *Chem. - Eur. J.*, 2013, **19**, 10911.

17 S. K. Yang, X. Shi, S. Park, S. Doganay, T. Ha and S. C. Zimmerman, *J. Am. Chem. Soc.*, 2011, **133**, 9964.

18 B. Gao, H. Li, H. Liu, L. Zhang, Q. Bai and X. Ba, *Chem. Commun.*, 2011, **47**, 3894.

19 Z. Xu, B. He, J. Shen, W. Yang and M. Yin, *Chem. Commun.*, 2013, **49**, 3646.

20 A. T. Zill, K. Licha, R. Haag and S. C. Zimmerman, *New J. Chem.*, 2012, **36**, 419.

21 Y. Chen, L. Zhou, Y. Pang, W. Huang, F. Qiu, X. Jiang, X. Zhu, D. Yan and Q. Chen, *Bioconjugate Chem.*, 2011, **22**, 1162.

22 G. Wang, H. Yin, J. C. Y. Ng, L. Cai, J. Li, B. Z. Tang and B. Liu, *Polym. Chem.*, 2013, **4**, 5297.

23 Y. Gao, G. Gao, Y. He, T. Liu and R. Qi, *Mini-Rev. Med. Chem.*, 2008, **8**, 889.

24 A. Ghilardi, D. Pezzoli, M. C. Bellucci, C. Malloggi, A. Negri, A. Sganappa, G. Tedeschi, G. Candiani and A. Volonterio, *Bioconjugate Chem.*, 2013, **24**, 1928.

25 J. S. Choi, K. Nam, J.-y. Park, J.-B. Kim, J.-K. Lee and J.-s. Park, *J. Control. Release*, 2004, **99**, 445.

26 M. Chen and M. Yin, *Prog. Polym. Sci.*, 2014, **39**, 365.

27 H.-A. Klok, J. R. Hernández, S. Becker and K. Müllen, *J. Polym. Sci. Part A: Polym. Chem.*, 2001, **39**, 1572.

28 Y.-Z. You, J.-J. Yan, Z.-Q. Yu, M.-M. Cui, C.-Y. Hong and B.-J. Qu, *J. Mater. Chem.*, 2009, **19**, 7656.

29 Y.-Z. You, Z.-Q. Yu, M.-M. Cui and C.-Y. Hong, *Angew. Chem. Int. Ed.*, 2010, **49**, 1099.

30 B. Zhang, X. Ma, W. Murdoch, M. Radosz and Y. Shen, *Biotechnol. Bioeng.*, 2013, **110**, 990.

31 J. Li, K. Guo, J. Shen, W. Yang, and M. Yin, *Small*, DOI: 10.1002/smll.201302920.

32. M. Yin, J. Shen, W. Pisula, M. Liang, L. Zhi and K. Müllen, *J. Am. Chem. Soc.*, 2009, **131**, 14618.

33 W. Qu, S. Chen, S. Ren, X. Jiang, R. Zhuo and X. Zhang, *Chin. J. Polym. Sci.*, 2013, **31**, 713.

34 X. Zhang, D. Luo, G. O. Pflugfelder and J. Shen, *Development*, 2013, **140**, 2917.